Published in final edited form as:
Gene Ther. 2009 July ; 16(7): 916–926. doi:10.1038/gt.2009.61.

Intravitreal delivery of AAV8 retinoschisin results in cell type-specific gene expression and retinal rescue in the *Rs1*-KO mouse

TK Park[1], **Z Wu**[2], **S Kjellstrom**[1], **Y Zeng**[1], **RA Bush**[1], **PA Sieving**[1,3], and **P Colosi**[2]

[1]Section for translational Research in Retinal and Macular Degeneration (STRRMD), National Institute on Deafness and Other Communication Disorders (NIDCD), National Institutes of Health (NIH), Bethesda, MD, USA

[2]Ocular Gene Therapy Laboratory, National Eye Institute (NEI), National Institutes of Health (NIH), Rockville, MD, USA

[3]National Eye Institute (NEI), National Institutes of Health (NIH), Bethesda, MD, USA

Abstract

X-linked juvenile retinoschisis (XLRS) is a neurodevelopmental abnormality caused by retinoschisin gene mutations. XLRS is characterized by splitting through the retinal layers and impaired synaptic transmission of visual signals resulting in impaired acuity and a propensity to retinal detachment. Several groups have treated murine retinoschisis models successfully using adeno-associated virus (AAV) vectors. Owing to the fragile nature of XLRS retina, translating this therapy to the clinic may require an alternative to invasive subretinal vector administration. Here we show that all layers of the retinoschisin knockout (*Rs1*-KO) mouse retina can be transduced efficiently with AAV vectors administered by simple vitreous injection. Retinoschisin expression was restricted to the neuroretina using a new vector that uses a 3.5-kb human retinoschisin promoter and an AAV type 8 capsid. Intravitreal administration to *Rs1*-KO mice resulted in robust retinoschisin expression with a retinal distribution similar to that observed in wild-type retina, including the expression by the photoreceptors lying deep in the retina. No off-target expression was observed. *Rs1*-KO mice treated with this vector showed a decrease in the schisis cavities and had improved retinal signaling evaluated by recording the electroretinogram 11–15 weeks after the application.

Keywords

retinoschisis; AAV vector; promoter; intravitreal injection

Introduction

X-linked juvenile retinoschisis (XLRS) is a neurodevelopmental retinal abnormality that manifests early in life and causes impaired acuity and a propensity to retinal detachment. XLRS is characterized by structural abnormalities in normal lamination of the retinal neuronal and plexiform layers. Clinical examination shows microcysts within the macula, and schisis or internal dissection of the layers of the peripheral retina,[1,2] and this is evident by using ocular coherence tomography.[3,4]

Correspondence: Dr P Colosi, Ocular Gene Therapy Laboratory, National Eye Institute, National Institutes of Health, 5626 Fishers Lane, Room 1S-16, Rockville, MD 20852, USA. colosip@nei.nih.gov.

Impaired retinal synaptic transmission of neural signals causes loss of dark-adapted absolute visual perception. This is evident on clinical electroretinogram (ERG) testing as a characteristic reduction of the b-wave response (from second-order retinal bipolar cells) relative to the photoreceptor a-wave, which frequently gives rise to an 'electronegative ERG waveform'.[5]

The fragile XLRS retina is more prone to disease-related complications, such as vitreous hemorrhage and retinal detachment, and the condition worsens with age.[6,7] The rate of retinal detachment in the XLRS population is considerably higher than in the general population (10 vs 0.01%, respectively),[8,9] and the post-operative outcome is much worse.[10,11]

X-linked juvenile retinoschisis is caused by mutations in the gene-encoding retinoschisin, a 224 amino acid secreted protein that is expressed only by the retina[12] and pineal.[13] Human retinoschisin is composed of a 23 amino-acid signal sequence, a 39 amino-acid Rs1 domain, a 157 amino-acid discoidin domain and a 5 amino-acid C-terminal segment. Discoidin domain-containing proteins are widely distributed in eukaryotes and mediate a variety of functions, including cell adhesion, cell–extracellular matrix interactions, signal transduction, phagocytosis of apoptotic cells, axon guidance, angiogenesis and blood clotting.[14] Many of these proteins are involved in extracellular matrix or cell binding, although some bind ligands such as vascular endothelial growth factor and semaphorin.

Retinoschisin is secreted from retinal neurons as a disulfide-linked homo-octameric complex, which adheres to the cell surface, but its function is not well understood.[15] Biochemical activities attributed to retinoschisin are the binding of β-2-laminin, αβ-crystallin, phospholipid, galactose and Na/K ATPase–SARM1 complex.[16–19] Retinoschisin is first observed in the mouse retina on postnatal day 1. During development, all retinal neurons express retinoschisin after differentiation, beginning with the ganglion cells, which are the first to mature, followed by neurons of each of the more distal layers. From P14 onward, it is strongly expressed in the outer half of the inner nuclear layer and by photoreceptor inner segment. All classes of retinal neurons, except horizontal cell, are shown to be labeled with retinoschisin antibody in adults.[20]

X-linked retinal diseases are particularly amenable to gene transfer-based therapies. Gene therapy for ocular disease has a set of attractive attributes, including a small tissue target and a closed compartment, which thereby requires a low dose. Additionally the retina is a relatively immune privileged environment. Multiple groups have used adeno-associated virus (AAV) retinoschisin vectors to complement the mutations of mice harboring retinoschisin gene deletions.[21,22] Retinal transduction with these vectors resulted in significant levels of retinoschisin protein in all layers of the retina, and improvement of the disease phenotype, including restoration of the normal positive ERG b-wave and a reduction of the cyst-like structures that are characteristic of the disease. The therapeutic effect was durable and persisted throughout the life of the animal.

An important precedent was recently set for the application of AAV vector-based ocular gene therapies to the clinic. Three separate groups evaluated the clinical use of AAV vectors for the treatment of another X-linked retinopathy, Leber congenital amaurosis (LCA) because of congenital retinal pigment epithelium (RPE) 65 deficiency.[23–25] AAV vectors expressing RPE65 were administered by subretinal injection to a total of nine subjects with LCA. The nine subjects comprised the collective low-dose cohorts of the three studies, each of which have a dose-escalation design. The majority of the treated subjects showed evidence of improvement in retinal function, visual acuity or reduction in nystagmus despite their relatively advanced state of retinal degeneration. Importantly, no vector-related adverse events were reported. These encouraging results provide the foundation for the clinical development of AAV vector-based therapeutics for the treatment of XLRS.

The LCA trials used subretinal injection to deliver the vector. This delivery strategy may be problematic for an XLRS trial, as subretinal injection gives geographically localized delivery.[25] Retinoschisin is expressed throughout the retina and optimal treatment of the disease will require transduction of the entire retina. Vector delivery by subretinal injection is limited maximally to ~25% of the retinal area. Although this amount of transduction is sufficient to cover the vicinity of the macula, much of the retina would probably not be transduced, and the untreated area would remain susceptible to retinal detachment and vitreous hemorrhage, which are the major causes of vision loss with this disease. Some additional spread of retinoschisin has been reported in retinas of mice transduced by subretinal injection, but it is not clear how this might scale to human subjects.[22] Subretinal injection of retinas with schisis pathology may be challenging and pose a significant risk to the visual function of the subject. Vitrectomy is usually carried out before subretinal injection. Adhesion of the vitreous to the retina may cause further laminar splitting of the fragile XLRS retina when the surgeon attempts to separate the vitreous from the retina. In addition, the injection itself may also be difficult. If the tip of the injection needle is not positioned deep enough, vector solution may be inadvertently routed into the schisis cavities and exacerbate the intraretinal splitting. An alternative vector administration method would be attractive for XLRS subjects.

In this study, we describe a method of obtaining efficient AAV vector-mediated gene transfer to XLRS retinas without the use of subretinal injection. We show that all layers of the retinoschisin knockout (*Rs1*-KO) mouse retina can be efficiently transduced with AAV type 8 (AAV8) vectors when administered by simple vitreous injection. This phenomenon appears specific to *Rs1*-KO mouse retina, as we did not observe similar outcome with wild-type retinas, nor do earlier reports indicate successful transduction of deep retinal layers following intravitreal application.[26,27]

We developed an AAV vector to complement vitreal administration. The vector was composed of a 3.5-kb human retinoschisin promoter, a human retinoschisin cDNA containing a truncated retinoschisin first intron, the human β-globin polyadenylation site and AAV type 2 (AAV2) inverted terminal repeats, packaged in an AAV type 8 capsid. Intravitreal administration of this vector to *Rs1*-KO mice resulted in robust retinoschisin expression with a retinal distribution that was similar to that observed in wild-type retina. Immunolabeling was specific to the retinoschisin-expressing cells of the retina with little or no off-target expression in other eye structures, such as the optic nerve, uveal tissue and cornea. *Rs1*-KO mice treated with this vector showed a decrease in number of and size of the schisis cavities and ERG improvement.

Results

Intravitreal administration of AAV vectors results in efficient transduction of all layers of the *Rs1*-KO mouse retina

Intravitreal injection was evaluated as a method of AAV vector delivery in wild-type and *Rs1*-KO mice. A dose of 1.5×10^{11} vector genomes (vg) of an AAV8 cytomegalovirus immediate early promoter-driven enhanced green fluorescent protein (AAV8 CMV EGFP) vector was administered to 8-week-old wild-type or *Rs1*-KO mice by intravitreal injection. An injection volume of 1.5 μl was used. The animals were killed 8 weeks later and retinal sections were examined for vector expression by fluorescent microscopy. Wild-type retinas showed little vector expression except for a few scattered cells. In contrast, retinas from *Rs1*-KO mice showed substantial EGFP expression in several retinal layers, including the RPE, photoreceptor cells, cells in the inner nuclear layer and ganglion cells (Figures 1a–d). AAV8 CMV EGFP was administered to *Rs1*-KO mice at 7 months of age to determine the effect of age on transduction efficiency of AAV vector delivered by the intravitreal route. The mice were killed 8 weeks later and examined for retinal EGFP expression. EGFP expression was observed,

which was similar to that seen in the younger animals, but some-what less efficient (Figures 1e and f).

Expression was most intense in the photoreceptor layer. EGFP expression was also seen in the optic nerve, ciliary body and peripheral cornea, indicating vector transduction of non-retinal structures and structures that do not express retinoschisin (Figures 1g–j).

Specific retinoschisin expression

Intravitreal administration of AAV8 CMV EGFP vector to *Rs1*-KO mice resulted in gene expression in multiple ocular structures. Some of these structures do not express retinoschisin in wild-type animals, including the optic nerve, the ciliary bodies, the peripheral cornea and the RPE. This widespread expression pattern is because of the broad cell tropisms of the AAV8 capsid and the CMV promoter. In order to restrict vector expression to cell types that express retinoschisin in wild-type animals, an AAV vector was constructed in which the human retinoschisin promoter was used to drive the expression of a human retinoschisin cDNA. The vector was composed of a 3429 bp human retinoschisin promoter, a human retinoschisin cDNA containing a 150 bp truncated retinoschisin first intron, the human β-globin polyadenylation site and AAV type 2 inverted terminal repeats (Figure 2). The promoter region was derived from the 4050 bp region of human genomic DNA that immediately precedes the retinoschisin translational start codon. This region was selected because it is rich in putative transcriptional regulatory motifs that are relatively conserved in mammals. The promoter fragment used for the construction has a 626 bp deletion of genomic repetitive sequence, which corresponds to base pairs −1286 to −1911 relative to the translational start codon. The deleted sequence encodes a primate-specific, short interspersed nuclear element and was removed to reduce the promoter size. Similarly, the truncated retinoschisin first intron and the small (218 bp) but efficient human β-globin 3′ untranslated region and polyadenylation site were used because of vector size considerations. The entire packaged vector is 4790 bp in length. This human retinoschisin vector was packaged in an AAV8 capsid and designated AAV8-hRSp4. It was tested for function and specificity in *Rs1*-KO mice.

Adeno-associated virus type 8-hRSp4 vector was administered to 6–7-week-old *Rs1*-KO mice by intravitreal injection at a dose of 7.5×10^{10} vg per eye. Retinas were examined 8 and 11 weeks later for retinoschisin expression by immunohistochemical methods using an earlier described retinoschisin antibody.[13,20,21,28,29] Wide lateral retinal expression was seen at both time points (Figures 3a and b). At 8 weeks after injection, retinoschisin staining was limited to the inner segments of the photoreceptors (Figure 3c). By 11 weeks after injection, retinoschisin staining was detected throughout the outer nuclear layer, the inner nuclear layer and the inner plexiform layer. However, retinoschisin staining was limited to the axonal endings of bipolar cells; the ganglion cell and retinal nerve fiber layers were not stained (Figure 3d).

Figure 4 compares the retinal structures and retinoschisin expression patterns of untreated *Rs1*-KO mice (Figure 4a) and wild-type mice (Figure 4b), with those of AAV8-hRSp4 vector-treated *Rs1*-KO mice (Figure 4f), at 17–18 weeks of age. AAV8-hRSp4 vector-treated *Rs1*-KO mice received 7.5×10^{10} vg per eye. Retinas from *Rs1*-KO mice receiving 2.3×10^{10} vg of AAV type 2 CMV mouse retinoschisin (AAV2 CMV mRS), an earlier studied vector,[21] were also examined for comparison (Figure 4d). In the earlier study, the AAV2 CMV mRS vector administered at this dose to *Rs1*-KO mice mediated the improvement of the electonegative ERG b-wave form that is characteristic of this animal model and the XLRS condition in humans. The vectors were administered to 6–7-week-old *Rs1*-KO mice by intravitreal injection 11 weeks before sacrifice. Retinoschisin staining was absent in the untreated *Rs1*-KO retina and 4′,6-diaminidino-2-phenylindol (DAPI) staining showed multiple large schisis cavities. Vector treated animals showed extensive retinoschisin staining in

multiple retinal layers and reduced schisis pathology. The retinoschisin staining patterns of the AAV8-hRSp4 and AAV2 CMV mRS vector-treated *Rs1*-KO mice were grossly similar to those of the wild-type mice with more pronounced staining of the inner segments and inner and outer plexiform layers in all the three cases.

Rs1-KO mice receiving AAV8-hRSp4 and AAV2 CMV mRS vectors were also examined at 8 weeks after injection. At this earlier time point, the expression patterns differed. AAV2 CMV mRS vector transduction resulted in retinoschisin expression in multiple retinal layers, including the inner segment of photoreceptor cells, outer nuclear layer and inner nuclear layer (Figure 4c). In contrast, AAV8-hRSp4 vector mediated expression in the inner segment of the photoreceptor exclusively (Figure 4e).

The ocular tissues that do not normally express retinoschisin were screened in *Rs1*-KO mice receiving intravitreal injections of AAV8-hRSp4 and AAV2 CMV mRS vectors. These included the optic nerve, retinal nerve fiber layer, ciliary bodies and the peripheral cornea. The AAV2 CMV mRS vector-treated mice showed expression in the optic nerve and the RFNL, but not in the ciliary body or peripheral cornea (Figure 5a). The AAV8-hRSp4 vector showed no expression in the optic nerve, retinal fiber layer, peripheral cornea or ciliary body (Figure 5b).

Functional improvement after vector administration

The effect on retinal function after intravitreal administration of the vector to *Rs1*-KO mice was evaluated in two prospective experiments. Dark-adapted ERG responses were recorded and visual signal transmission between the photoreceptors and the bipolar cell second-order neurons was evaluated through the b/a-wave ratio for stimuli of 0.6 log cd-s m^{-2} flash intensity. Reduction in this ratio is characteristic of the clinical ERG recorded from XLRS patients. The b-wave reflects responses of bipolar cells, and the a-wave reflects responses of photoreceptor cells. Photoreceptor number is often reduced in *Rs1*-KO mice, and the ratio of the b-wave to a-wave normalizes the second-order neuron response to the input from photoreceptors.

In the first experiment, the vector was administered to eight eyes of four adult *Rs1*-KO male mice at about 7 weeks of age, and ERGs were recorded 11 weeks later. ERGs from six untreated eyes of three *Rs1*-KO male mice served as controls. All mice that entered the study were evaluated at the end (Table 1, Figure 6). The mean b/a-wave ratio was larger in the treated versus untreated eyes ($P = 0.04$, Student's two-tailed *t*-test).

As the control mice in experiment 1 were 3 weeks older than the treated mice when evaluated, we conducted a second experiment in which the vector was administered to one eye of six adult *Rs1*-KO male mice, and the untreated fellow eyes of these mice served as controls. Injections were done at about 7 weeks of age, and ERGs were recorded from both eyes 15 weeks later. One mouse died during anesthesia induction before the ERG could be recorded and provided no data. The b/a-wave ratio in four of the five remaining mice was greater in the treated eye compared with the paired untreated eye (Table 2, Figure 6). Statistical analysis of treated versus untreated eyes by group gave $P < 0.012$ (Student's two-tailed *t*-test, $n = 5$ for each group).

Discussion

This study demonstrates that intravitreal injection of an AAV vector with a retinoschisin promoter results in efficient and tissue-specific expression of retinoschisin in a mouse model of X-linked retinoschisis. The clinical feasibility of AAV vector-based gene therapy for human ocular retinal diseases was recently validated by the encouraging results from three trials that assessed the safety and performance of AAV vectors to treat LCA from *RPE65* gene mutations. All these trials used subretinal injections for vector administration and is the only method of

retinal vector administration that has been vetted in the clinic.[23–25] However, as XLRS disease impairs the structural integrity of the retina, vitreal injection for retinoschisin gene administration would be substantially safer in the clinic than subretinal injection, which requires retinal surgical manipulation and vitrectomy.[23–25] Vitreal injection is routinely used for clinical ocular therapeutics and would be an attractive alternative for AAV gene therapeutics to treat XLRS if it was possible.

Intravitreal injection of the AAV8 CMV EGFP reporter vector resulted in the transduction of multiple layers of the *Rs1*-KO mouse retina, including the RPE, photoreceptor cells, cells in the inner nuclear layer and ganglion cells. All retinal layers that express retinoschisin in wild-type animals showed reporter gene expression. Expression was also seen in non-retinal tissues, including the optic nerve, ciliary body and peripheral cornea. *Rs1*-KO mice ranging in age from 6 to 39 weeks responded similarly to reporter vector administered by vitreal injection. In contrast, the retinas from wild-type animals showed very little expression after intravitreal vector administration.

To restrict expression to the cell types that produce retinoschisin in wild-type animals, a vector was constructed in which a 3.5-kb fragment of the human retinoschisin promoter was used to drive expression of a human retinoschisin cDNA. Vitreal administration of this vector packaged in an AAV8 capsid produced a wide lateral spread of retinoschisin in XLRS retina with a distribution among the retinal layers that was roughly similar to wild-type retina. Retinoschisin staining in the optic nerve, ciliary body and peripheral cornea was notably absent. *Rs1*-KO mice treated with this vector showed reduced retinal schisis pathology.

Retinoschisin protein accumulated slowly in the retina of retinoschisin vector-treated *Rs1*-KO mice. Retinal retinoschisin levels had not peaked 8 weeks after injection for either the AAV2 CMV mRS vector or the AAV8-hRSp4 vector. At this time point, the AAV2 CMV mRS vector produced retinoschisin accumulation in multiple retinal layers, whereas the AAV8-hRSp4 vector produce accumulation only in the inner segment layer. The reason for the difference is not clear but may have to do with the differences in tropisms of the promoters and capsids of the two vectors. After 11 weeks, the retinoschisin levels of the retinas transduced by both vectors appeared grossly similar to wild-type retinas in quantity and distribution. Our data do not allow us to conclude whether the spread of retinoschisin through the retina during this accumulation phase was mainly because of the local synthesis, or whether secretion and transport from producing retinal layers to other retinal layers also played a major role.

Functional ERG evaluation of the XLRS eyes after intravitreal administration of the AAV8-hRSp4 vector showed rescue of the b-wave relative to the a-wave in two independent experiments with XLRS-affected mice. The improved b/a-wave ratio following provision of retinoschisin fits well with the restoration of synaptic integrity in the *Rs1*-KO mouse retina that we observed earlier following AAV2 CMV mRS vector delivered to 14-day-old eyes by intravitreal injection.[28] That study observed better synaptic OPL organization and the presence of the synaptic proteins PSD95 and mGluR6 by western blot analysis, along with enhanced b-wave amplitude and improved b/a-wave ratio in 8-month-old mice. GFAP protein expression was also reduced as a sign of a diminished retinal injury response in treated eyes. This study demonstrates the efficacy of vector administration by intravitreal injection in adult *Rs1*-KO mice.

The b/a-wave ratio reflects signal transmission between rod photoreceptors (a-wave) and the post-synaptic bipolar cell neurons (b-wave). This ratio is characteristically reduced in XLRS disease. In about one-third of the cases, the ERG shows an ‘electronegative waveform’ configuration because the positive-going b-wave fails to rise back to or above baseline from the initial negative a-wave component.[30] Although the b-wave amplitude normally is greater

than the a-wave in the dark-adapted ERG for bright stimuli, the b-wave characteristically is reduced in XLRS disease.[5] Considerable ERG variability is observed, however,[30,31] and even the a-wave is diminished in some portion of XLRS affected males, possibly in up to one-third of the cases.[30] The *Rs1*-KO disease process certainly involves the rod photoreceptors in these XLRS mouse models.[22,29] Hence, using the b/a-wave ratio and normalizing the bipolar cell b-wave signaling by the a-wave helps to account for abnormalities originating with the rod photoreceptors.

The absence of retinoschisin protein causes a striking change in the properties of the retina. Wild-type murine retinas are not permeable to AAV vectors. This lack of permeability is not dependent on AAV serotype and has been observed with vectors made with capsids from AAV types 2, 5, 7, 8 and 9.[26] Vectors made from all serotypes tested so far are able to penetrate all retinal layers of *Rs1*-KO mice and will even transduce the retinal pigment epitheluim. These include vectors made with capsids from AAV types 2, 5 and 8 (AAV5 data not shown).[21] All of these capsids have diameters of ~28 nm but significantly differ in their amino-acid sequence, surface-exposed amino acids and surface charge.[32–34] The lack of retinoschisin seems to significantly change the properties of the interstitial matrix making the retina permeable to particles that are at least 28 nm in diameter. Retinal permeability to AAV vectors is uniform across the *Rs1*-KO retina and is not localized to regions showing schisis pathology.

The porosity of the *Rs1*-KO retina may have an effect on protein compartmentalization in the retina. For example, the interphotoreceptor retinoid-binding protein (IRBP) is thought to be sequestered within the subretinal space because of its large size (Stokes' radius = 5.5 nm).[35] In *Rs1*-KO retina, 28 nm AAV vector particles can traverse the subretinal space and transduce RPE. Consequently, IRBP may not be restricted to the subretinal space in *Rs1*-KO mouse. Other soluble proteins in the vitreous, subretinal space and retina may be dislocated in retinoschisis as well. Whether or not abnormal retinal porosity contributes to the retinoschisis phenotype remains to be investigated.

Materials and methods

Constructions

All AAV vector constructions used AAV2 inverted terminal repeats. The expression cassette of the AAV8 cytomegalovirus-enhanced green fluorescent protein vector (AAV8 CMV EGFP) consisted of a CMV immediate early promoter, a chimeric CMV/human β-globin intron, the EGFP gene and a human β-globin polyadenylation site. The AAV2 CMV mouse retinoschisin vector (AAV2 CMV mRS) was described earlier.[21] The expression cassette consists of a CMV promoter, a chimeric β-globin/immunoglobulin G intron, a mouse retinoschisin cDNA and an SV40 late polyadenylation site. The AAV8-hRSp4 vector was composed of a 3429 bp human retinoschisin promoter, a human retinoschisin cDNA containing a 150-bp truncated retinoschisin first intron and the human β-globin polyadenylation site. The promoter region was derived from a 4050 bp region of human genomic DNA that immediately precedes the retinoschisin translational start codon. The promoter fragment used for the construction has a 626 bp deletion of genomic repetitive sequence, which corresponds to base pairs −1286 to −1911 relative to the translational start codon.

Adeno-associated virus vectors

Adeno-associated virus vectors were produced by the triple transfection method and purified by polyethylene glycol precipitation followed by cesium chloride density gradient fractionation. The method has been described earlier.[36] The purified vectors were formulated in 10 mM Tris–HCl, 180 mM NaCl, pH 7.4 and stored at −80 °C before use. Quantification of vectors was done by real-time PCR using linearized plasmid standards.

Intravitreal injections

Experimental procedures were reviewed and approved by the Animal Care and Use Committee of NEI, NIH. *Rs1*-KO ($Rs1^{-/y}$) mice of 6–7-week-old and 7-month-old were used in this study. All mice were back-crossed more than ten generations onto C57BL/6 background and genotyped by PCR amplification using tail DNA. Age-matched C57BL/6 mice used as controls were obtained from the Jackson Laboratory (Bar Harbor, ME, USA).

To evaluate retinal transduction after vitreal administration of AAV8 CMV EGFP vector, four 6–7–week-old *Rs1*-KO mice, three 7–month-old *Rs1*-KO mice and eight 8-week-old wild-type mice were used.

To evaluate the expression of AAV2 CMV mRS and AAV8-hRSp4 vectors administered by intravitreal injection, 17 6–7-week-old *Rs1*-KO mice were used.

After anesthetizing animals with intraperitoneal ketamine (80 mg kg^{-1})/xylazine (15 mg kg^{-1}), both eyes of each mouse were dilated with 2.5% phenylephrine hydrochloride (Bausch & Lomb Inc., Tampa, FL, USA) and 0.5% tropicamide (Alcon Laboratories, Inc., Fort Worth, TX, USA). Intravitreal injection was performed using a 5-μl Hamilton syringe with 33-gauge beveled-tip needle (Hamilton, Reno, NV, USA). The needle was inserted through the sclera just posterior to the limbus in the temporal side of the eye. Solutions were slowly injected into the vitreous cavity. The needle was held in place for 30 s after injection, whereas the intraocular pressure equilibrated. Three age-matched wild-type mice and untreated *Rs1*-KO mice were used as positive and negative control.

Histology

While killing, deep anesthesia was induced with ketamine (80 mg kg^{-1}) and xylazine (4 mg kg^{-1}), and the mice were perfused with 4% paraformaldehyde in 0.1 M phosphate buffer pH 7.4. Enucleated eyeballs were immersed in the same fixative overnight. To evaluate transgene expression in the uveal tissues and peripheral cornea, eyecups were prepared by cutting through the peripheral cornea, removing the iris and lens. The eyecups were subsequently rinsed in 0.1 M phosphate buffer pH 7.4 (PB). For frozen sections, the eyecups were immersed in 30% sucrose/0.1 M PB as a cryoprotectant and embedded in Tissue-Tek OCT compound (EM Sciences, Fort Washington, PA, USA). Thick sections of 8 μ were thaw-mounted onto poly-lysine-coated slides and stored at −80 °C until further processing. The sections were stained with DAPI.

The immunofluorescence labeling procedure employed an affinity-purified polyclonal rabbit antibody raised against a synthetic peptide corresponding to retinoschisin amino-acid residues 24–37 (stdegedpwyqka). This sequence is conserved in murine and human retinoschisin. The anti-retinoschisin antibody was visualized with an anti-rabbit IgG-tagged with Alexa 568 (red) (Invitrogen, Carlsbad, CA, USA) and the sections were counterstained with DAPI nuclear dye (blue). The frozen sections were also stained with hematoxylin–eosin for light microscopy. The sections shown in the figures are representative results.

Electroretinogram measurement

Two prospective experiments were conducted with *Rs1*-KO mice to evaluate retinal function after gene delivery using the AAV8-hRSp4 vector. Progeny from mating a heterozygous female *Rs1*-KO carrier with an unaffected C57/BL6 male (purchased from the Jackson Laboratories) were genotyped at 1 month of age to identify males carrying the *Rs1*-KO gene construction. Eyes were treated by inserting a 33-gauge needle into the vitreous cavity under direct visualization and injecting 1.5 μl of the AAV8-hRSp4 vector. The concentration of the

AAV8-hRSp4 vector stock was 5×10^{13} vg ml^{-1} and a dose of 7.5×10^{10} vg was administered per eye. Mice were maintained in 12/12 h cyclic lighting until ERGs were recorded.

Four *Rs1*-KO mice were used in the first experiment and received intravitreal injection in both eyes at 6–7 weeks of age. ERGs were recorded 11 weeks after from all eight eyes at 18 weeks of age. ERGs were recorded from six eyes of three untreated *Rs1*-KO mice at 21.1 weeks of age as controls. All ERGs were included in the analysis.

In a second experiment, six *Rs1*-KO mice received intravitreal injection in one eye at 7–8 weeks of age, and the untreated fellow eyes served as controls. ERGs were recorded simultaneously from both eyes of each animal 15–16 weeks later. One animal died during anesthesia before an ERG was recorded and gave no functional data. All data from the remaining five animals were included in the analysis.

For ERG recordings, mice were dark-adapted overnight for 12 h before intraperitoneal anesthesia with ketamine (80 mg kg^{-1}) and xylazine (4 mg kg^{-1}). Pupils were dilated with topical 0.5% tropicamide and 0.5% phenylephrine HCl. Mice were placed on a heating pad to maintain body temperature near 38 °C. Full-field scotopic ERGs were recorded from both eyes simultaneously by placing gold wire loop on each cornea with a drop of methylcellulose after 1% proparacaine topical anesthetic. Gold wires were placed on the sclera at the limbus as the differential electrodes, and a ground wire was attached to the left ear. Responses were elicited with xenon single flashes (Grass Photic Stimulator PS33, Astro-Med Inc., West Warwick, RI, USA) delivered in a Ganzfeld (full field) sphere. Responses were amplified 5000 times and filtered using a 0.1 Hz–1 kHz bandpass and 60 Hz line-frequency filter (CP511 AC amplifier, Grass Technologies, Astro-Med Inc.). A-waves were measured from the pre-stimulus baseline to the initial trough. B-waves were measured from the a-wave trough. The ratio of (b-wave/a-wave) was determined for responses to 0.6 log cd-s m^{-2} stimuli as is commonly used clinically to evaluate the 'electronegative' ERG response that characterizes human X-linked retinoschisis disease. [5,30,31] This intensity is also used to characterize the ERG of *Rs1*-KO mice.[21]

Acknowledgments

We thank Maria Santos for help with husbandry and Jinbo Li for help with histology.

References

1. Sikkink SK, Biswas S, Parry NR, Stanga PE, Trump D. X-linked retinoschisis: an update. J Med Genet 2007;44:225–232. [PubMed: 17172462]
2. Tantri A, Vrabec TR, Cu-Unjieng A, Frost A, Annesley WH Jr, Donoso LA. X-linked retinoschisis: a clinical and molecular genetic review. Surv Ophthalmol 2004;49:214–230. [PubMed: 14998693]
3. Prenner JL, Capone A Jr, Ciaccia S, Takada Y, Sieving PA, Trese MT. Congenital X-linked retinoschisis classification system. Retina 2006;26(7 Suppl):S61–S64. [PubMed: 16946682]
4. Minami Y, Ishiko S, Takai Y, Kato Y, Kagokawa H, Takamiya A, et al. Retinal changes in juvenile X linked retinoschisis using three dimensional optical coherence tomography. Br J Ophthalmol 2005;89:1663–1664. [PubMed: 16299154]
5. Peachey NS, Fishman GA, Derlacki DJ, Brigell MG. Psychophysical and electroretinographic findings in X-linked juvenile retinoschisis. Arch Ophthalmol 1987;105:513–516. [PubMed: 3566604]
6. George ND, Yates JR, Moore AT. X linked retinoschisis. Br J Ophthalmol 1995;79:697–702. [PubMed: 7662639]
7. Roesch MT, Ewing CC, Gibson AE, Weber BH. The natural history of X-linked retinoschisis. Can J Ophthalmol 1998;33:149–158. [PubMed: 9606571]
8. Sasaki K, Ideta H, Yonemoto J, Tanaka S, Hirose A, Oka C. Epidemiologic characterstics of rhegmatogenous retinal detachement in Kumamoto, Japan. Graefes Arch Clin Exp Ophthalmol 1995;233:772–776. [PubMed: 8626085]

9. Kellner U, Brümmer S, Foerster MH, Wessing A. X-linked congenital retinoschisis. Graefes Arch Clin Exp Ophthalmol 1990;228:432–437. [PubMed: 2227486]
10. Regillo CD, Tasman WS, Brown GC. Surgical management of complications associated with X-linked retinoschisis. Arch Ophthalmol 1993;111:1080–1086. [PubMed: 8352691]
11. Rosenfeld PJ, Flynn HW Jr, McDonald HR, Rubsamen PE, Smiddy WE, Sipperley JO, et al. Outcomes of vitreoretinal surgery in patients with X-linked retinoschisis. Ophthalmic Surg Lasers 1998;29:190–197. [PubMed: 9547772]
12. Sauer CG, Gehrig A, Warneke-Wittstock R, Marquardt A, Ewing CC, Gibson A, et al. Positional cloning of the gene associated with X-linked juvenile retinoschisis. Nat Genet 1997;17:164–170. [PubMed: 9326935]
13. Takada Y, Fariss RN, Muller M, Bush RA, Rushing EJ, Sieving PA. Retinoschisin expression and localization in rodent and human pineal and consequences of mouse RS1 gene knockout. Mol Vis 2006;12:1108–1116. [PubMed: 17093404]
14. Baumgartner S, Hofmann K, Chiquet-Ehrismann R, Bucher P. The discoidin domain family revisited: new members from prokaryotes and a homology-based fold prediction. Protein Sci 1998;7:1626–1631. [PubMed: 9684896]
15. Wu WW, Wong JP, Kast J, Molday RS. RS1, a discoidin domain-containing retinal cell adhesion protein associated with X-linked retinoschisis, exists as a novel disulfide-linked octamer. J Biol Chem 2005;280:10721–10730. [PubMed: 15644328]
16. Steiner-Champliaud MF, Sahel J, Hicks D. Retinoschisin forms a multi-molecular complex with extracellular matrix and cytoplasmic proteins: interactions with beta2 laminin and alphaB-crystallin. Mol Vis 2006;12:892–901. [PubMed: 16917482]
17. Vijayasarathy C, Takada Y, Zeng Y, Bush RA, Sieving PA. Retinoschisin is a peripheral membrane protein with affinity for anionic phospholipids and affected by divalent cations. Invest Ophthalmol Vis Sci 2007;48:991–1000. [PubMed: 17325137]
18. Molday LL, Wu WW, Molday RS. Retinoschisin (RS1), the protein encoded by the X-linked retinoschisis gene, is anchored to the surface of retinal photoreceptor and bipolar cells through its interactions with a Na/K ATPase-SARM1 complex. J Biol Chem 2007;282:32792–32801. [PubMed: 17804407]
19. Dyka FM, Wu WW, Pfeifer TA, Molday LL, Grigliatti TA, Molday RS. Characterization and purification of the discoidin domain-containing protein retinoschisin and its interaction with galactose. Biochemistry 2008;47:9098–9106. [PubMed: 18690710]
20. Takada Y, Fariss RN, Tanikawa A, Zeng Y, Carper D, Bush R, et al. A retinal neuronal developmental wave of retinoschisin expression begins in ganglion cells during layer formation. Invest Ophthalmol Vis Sci 2004;45:3302–3312. [PubMed: 15326155]
21. Zeng Y, Takada Y, Kjellstrom S, Hiriyanna K, Tanikawa A, Wawrousek E, et al. RS-1 gene delivery to an adult Rs1h knockout mouse model restores ERG b-wave with reversal of the electronegative waveform of X-linked retinoschisis. Invest Ophthalmol Vis Sci 2004;45:3279–3285. [PubMed: 15326152]
22. Min SH, Molday LL, Seeliger MW, Dinculescu A, Timmers AM, Janssen A, et al. Prolonged recovery of retinal structure/function after gene therapy in an Rs1h-deficient mouse model of x-linked juvenile retinoschisis. Mol Ther 2005;12:644–651. [PubMed: 16027044]
23. Maguire AM, Simonelli F, Pierce EA, Pugh EN Jr, Mingozzi F, Bennicelli J, et al. Safety and efficacy of gene transfer for Leber's congenital amaurosis. N Engl J Med 2008;358:2240–2248. [PubMed: 18441370]
24. Bainbridge JW, Smith AJ, Barker SS, Robbie S, Henderson R, Balaggan K, et al. Effect of gene therapy on visual function in Leber's congenital amaurosis. N Engl J Med 2008;358:2231–2239. [PubMed: 18441371]
25. Cideciyan AV, Aleman TS, Boye SL, Schwartz SB, Kaushal S, Roman AJ, et al. Human gene therapy for RPE65 isomerase deficiency activates the retinoid cycle of vision but with slow rod kinetics. Proc Natl Acad Sci USA 2008;105:15112–15117. [PubMed: 18809924]
26. Lebherz C, Maguire A, Tang W, Bennett J, Wilson JM. Novel AAV serotypes for improved ocular gene transfer. J Gene Med 2008;10:375–382. [PubMed: 18278824]

27. Natkunarajah M, Trittibach P, McIntosh J, Duran Y, Barker SE, Smith AJ, et al. Assessment of ocular transduction using single-stranded and self-complementary recombinant adeno-associated virus serotype 2/8. Gene Therapy 2008;15:463–467. [PubMed: 18004402]
28. Takada Y, Vijayasarathy C, Zeng Y, Kjellstrom S, Bush RA, Sieving PA. Synaptic pathology in retinoschisis knockout ($Rs1^{-/y}$) mouse retina and modification by rAAV-Rs1 gene delivery. Invest Ophthalmol Vis Sci 2008;49:3677–3686. [PubMed: 18660429]
29. Kjellstrom S, Bush RA, Zeng Y, Takada Y, Sieving PA. Retinoschisin gene therapy and natural history in the *Rs1h*-KO mouse: long-term rescue from retinal degeneration. Invest Ophthalmol Vis Sci 2007;48:3837–3845. [PubMed: 17652759]
30. Bradshaw K, George N, Moore A, Trump D. Mutations of the XLRS1 gene cause abnormalities of photoreceptor as well as inner retinal responses of the ERG. Doc Ophthalmol 1999;98:153–173. [PubMed: 10947001]
31. Sieving PA, Bingham EL, Kemp L, Richards J, Hiriyanna K. Juvenile X-linked retinoschisis from XLRS1 Arg213Trp mutation with preservation of the electroretinogram scotopic b-wave. Am J Ophthalmol 1999;128:179–184. [PubMed: 10458173]
32. Xie Q, Bu W, Bhatia S, Hare J, Somasundaram T, Azzi A, et al. The atomic structure of adeno-associated virus (AAV-2), a vector for human gene therapy. Proc Natl Acad Sci USA 2002;99:10405–10410. [PubMed: 12136130]
33. Walters RW, Agbandje-McKenna M, Bowman VD, Moninger TO, Olson NH, Seiler M, et al. Structure of adeno-associated virus serotype 5. J Virol 2004;78:3361–3371. [PubMed: 15016858]
34. Nam HJ, Lane MD, Padron E, Gurda B, McKenna R, Kohlbrenner E, et al. Structure of adeno-associated virus serotype 8, a gene therapy vector. J Virol 2007;81:12260–12271. [PubMed: 17728238]
35. Gonzalez-Fernandez F. Interphotoreceptor retinoid-binding protein: an old gene for new eyes. Vision Res 2003;43:3021–3036. [PubMed: 14611938]
36. Grimm D, Zhou S, Nakai H, Thomas CE, Storm TA, Fuess S, et al. Preclinical *in vivo* evaluation of pseudotyped adeno-associated virus vectors for liver gene therapy. Blood 2003;102:2412–2419. [PubMed: 12791653]

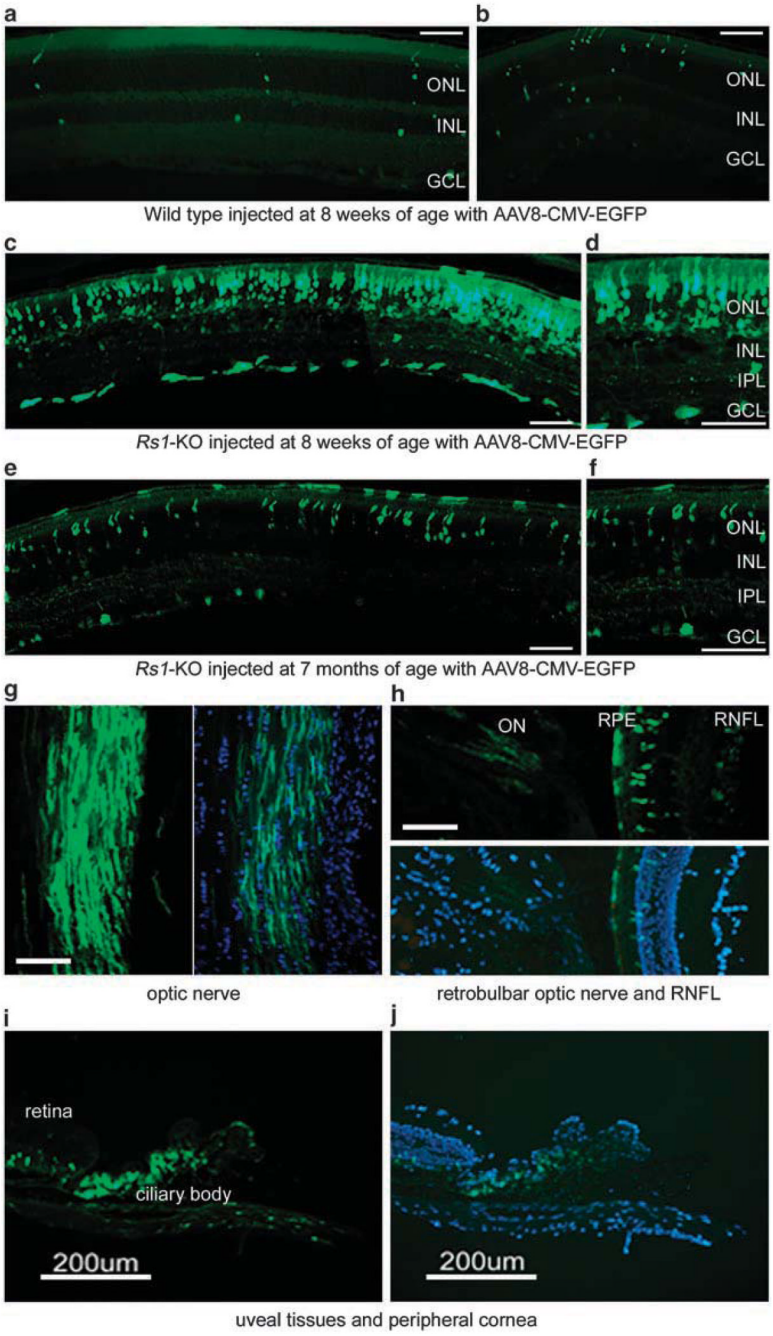

Figure 1.

Retinal enhanced green fluorescent protein (EGFP) expression after intravitreal injection of adeno-associated virus type 8 (AAV8) CMV EGFP vector. A dose of 1.5×10^{11} vg of AAV8 CMV EGFP vector was administered to wild-type (**a**, **b**) and retinoschisin knockout (*Rs1*-KO) mice (**c**, **d**) at 8 weeks of age, and older *Rs1*-KO mice (**e**, **f**) at 7 months of age. The mice were killed at 8 weeks post injection (PI) and ocular sections were prepared. EGFP expression (green) is shown in the retinal sections of the mice mentioned above (**a–f**), and in the optic nerve (**g**), retinal nerve fiber layer (RNFL) (**h**), ciliary body (**i**) and cornea (**j**) of *Rs1*-KO mice. ONL, outer nuclear layer; INL, inner nuclear layer; IPL, inner plexiform layer; GCL, ganglion cell layer. Calibration bar, 100 μm unless otherwise marked.

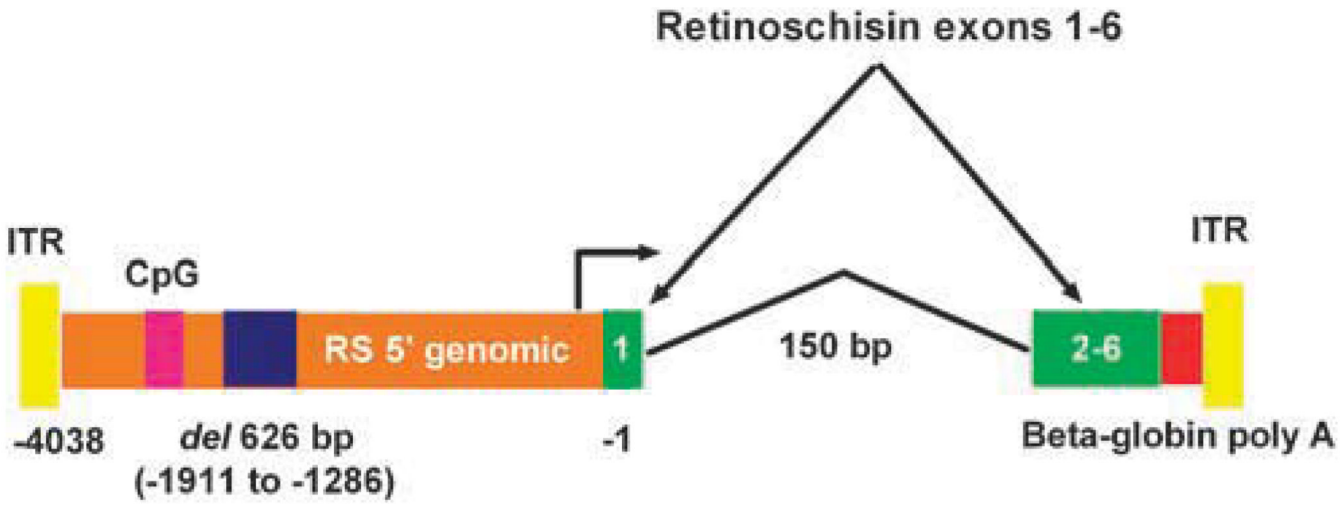

Figure 2.

Schematic illustration of the adeno-associated virus (AAV) 8-hRSp4 vector genome. A 3429 bp human retinoschisin promoter drives the expression of a human retinoschisin cDNA containing a 150 bp truncated retinoschisin first intron. The promoter fragment has a 626 bp deletion of genomic repetitive sequence, which corresponds to base pairs −1286 to −1911 relative to the translational start codon. A 218-bp fragment encoding the human β-globin 3′ untranslated region and polyadenylation site mediates polyadenylation. The inverted terminal repeats (ITRs) are derived from AAV2. CpG indicates a CpG island.

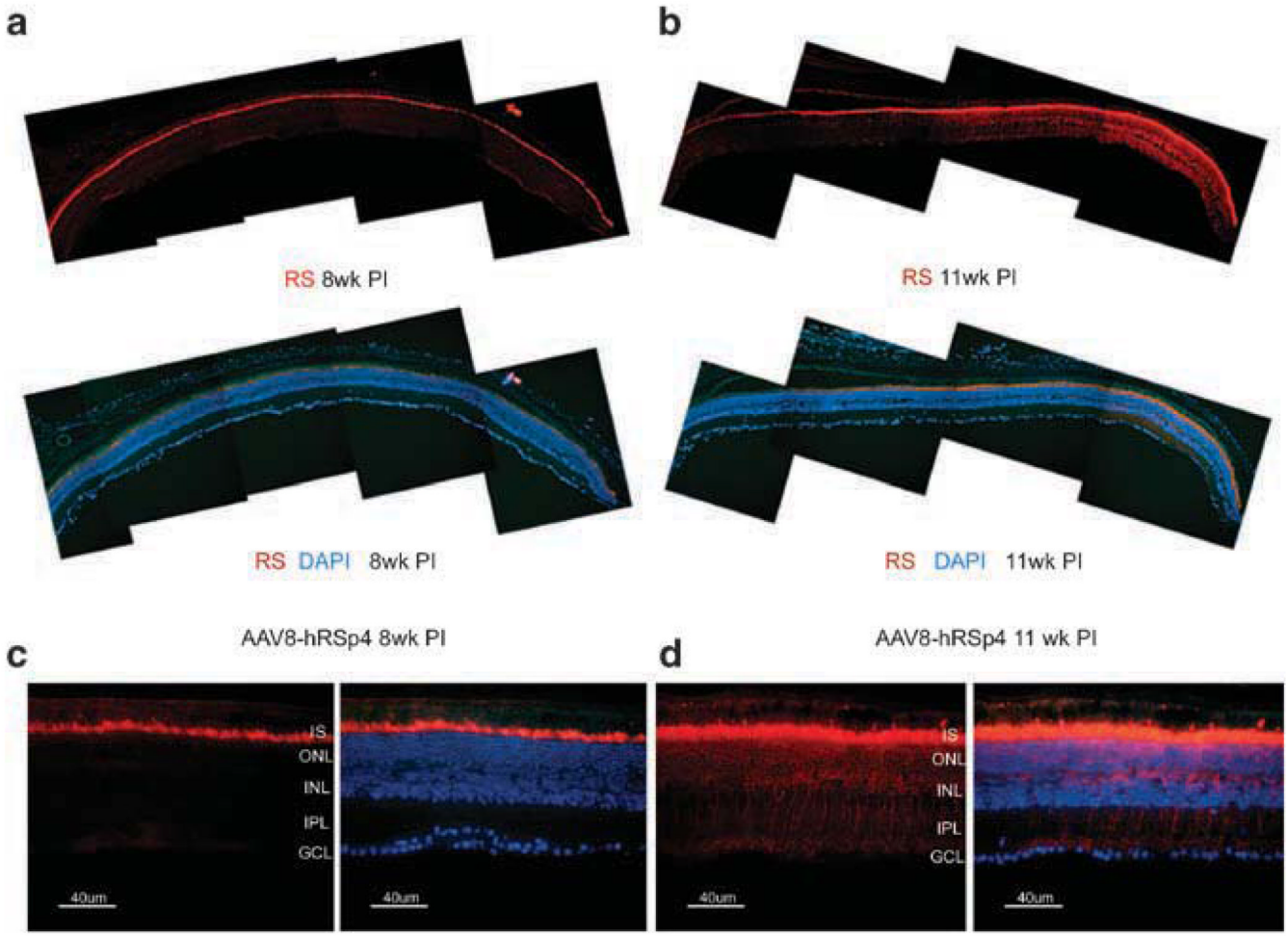

Figure 3.

Retinoschisin expression after vitreal administration of adeno-associated virus type 8 (AAV8)-hRSp4 vector to retinoschisin knockout (*Rs1*-KO) mice. *Rs1*-KO mice of 9-week-old received intravitreal injections of 7.5×10^{10} vg of AAV8-hRSp4 vector. Animals were killed at 8 and 11 weeks post injection and retinal sections were prepared. Fluorescence images were taken under low (×200) and high (×400) magnification. Immunolabeling of retinoschisin (RS) was visualized with Alexa-568-conjugated goat-anti-rabbit IgG (red). The nuclei were stained blue with 4′,6-diaminidino-2-phenylindole (DAPI) in some sections. IS, inner segment; ONL, outer nuclear layer; OPL, outer plexiform layer; INL, inner nuclear layer; IPL, inner plexiform layer; GCL, ganglion cell layer.

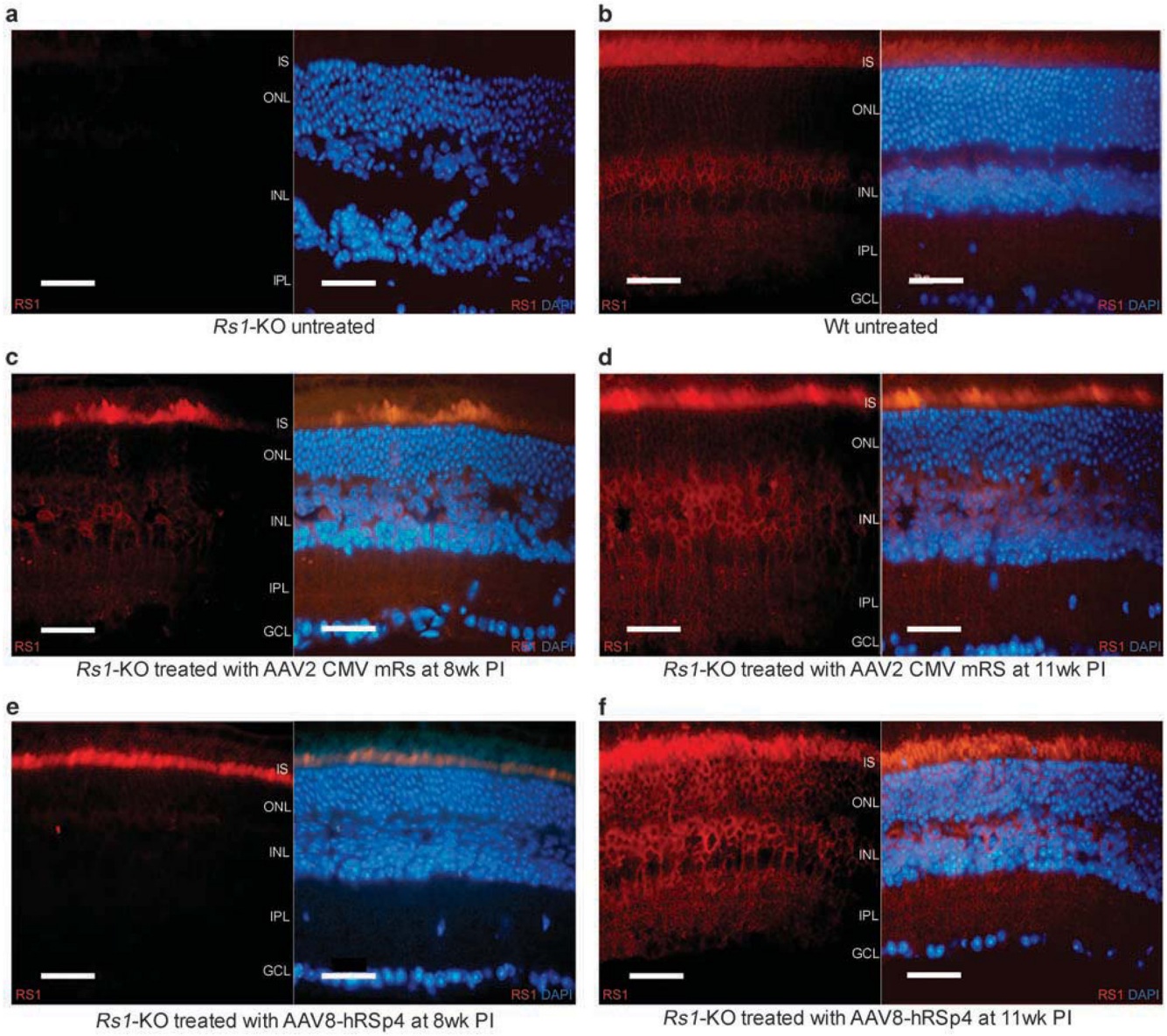

Figure 4.

Retinoschisin expression in wild-type (WT) mice, retinoschisin knockout (*Rs1*-KO) mice, and *Rs1*-KO mice treated with adeno-associated virus (AAV) 2 CMV mRS and AAV8-hRSp4 vectors. Vector treated mice received intravitreal injections of 2.3×10^{10} vg of AAV2 CMV mRS or 7.5×10^{10} vg of AAV8-hRSp4 at 9 weeks of age. Vector treated animals were killed at 8 and 11 weeks post injection (PI) (panels **c–f**). The untreated animals were killed at 20 weeks of age (panels **a** and **b**). Immunolabeling of retinoschisin (RS) was visualized with Alexa-568-conjugated goat-anti-rabbit IgG (red). Some sections were also stained with 4′,6-diaminidino-2-phenylindole (DAPI) to indicate nuclei (blue). IS, inner segments; ONL, outer nuclear layer; INL, inner nuclear layer; IPL, inner plexiform layer; GCL, ganglion cell layer; Wt, wild type. Calibration bar, 40 μm.

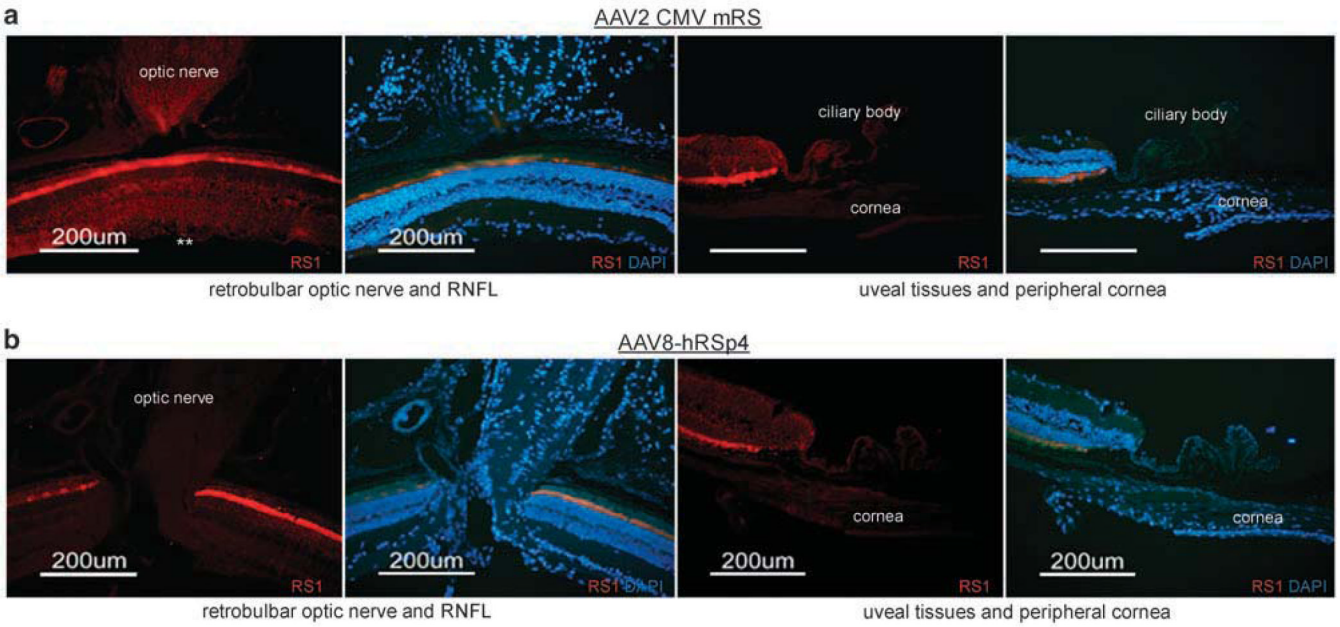

Figure 5.

Gene expression patterns in extra-retinal tissues intravitreal injection of adeno-associated virus (AAV) 2 CMV mRS and AAV8-hRSp4 vectors. Retinoschisin knockout mice of 9-week-old received intravitreal injections of AAV2 CMV mRS, and AAV8-hRSp4 vectors at doses of 2.3×10^{10} and 7.5×10^{10} vg per eye, respectively. AAV2 CMV mRS, and AAV8-hRSp4 vector-treated mice were killed at 11 weeks post injection. Immunolabeling of retinoschisin was visualized with Alexa-568-conjugated goat-anti-rabbit IgG (red). Some sections were also stained with 4′,6-diaminidino-2-phenylindole (DAPI) to indicate nuclei (blue). AAV2 CMV mRS-treated mice showed expression in the optic nerve and the retinal nerve fiber layer (RFNL), but not in the ciliary body or peripheral cornea (**a**). AAV8-hRSp4 vector-treated mice did not show retinoschisin expression in the optic nerve, RNFL or uveal tissue (**b**). Retinoschisin expression in RNFL was marked with double asterisk.

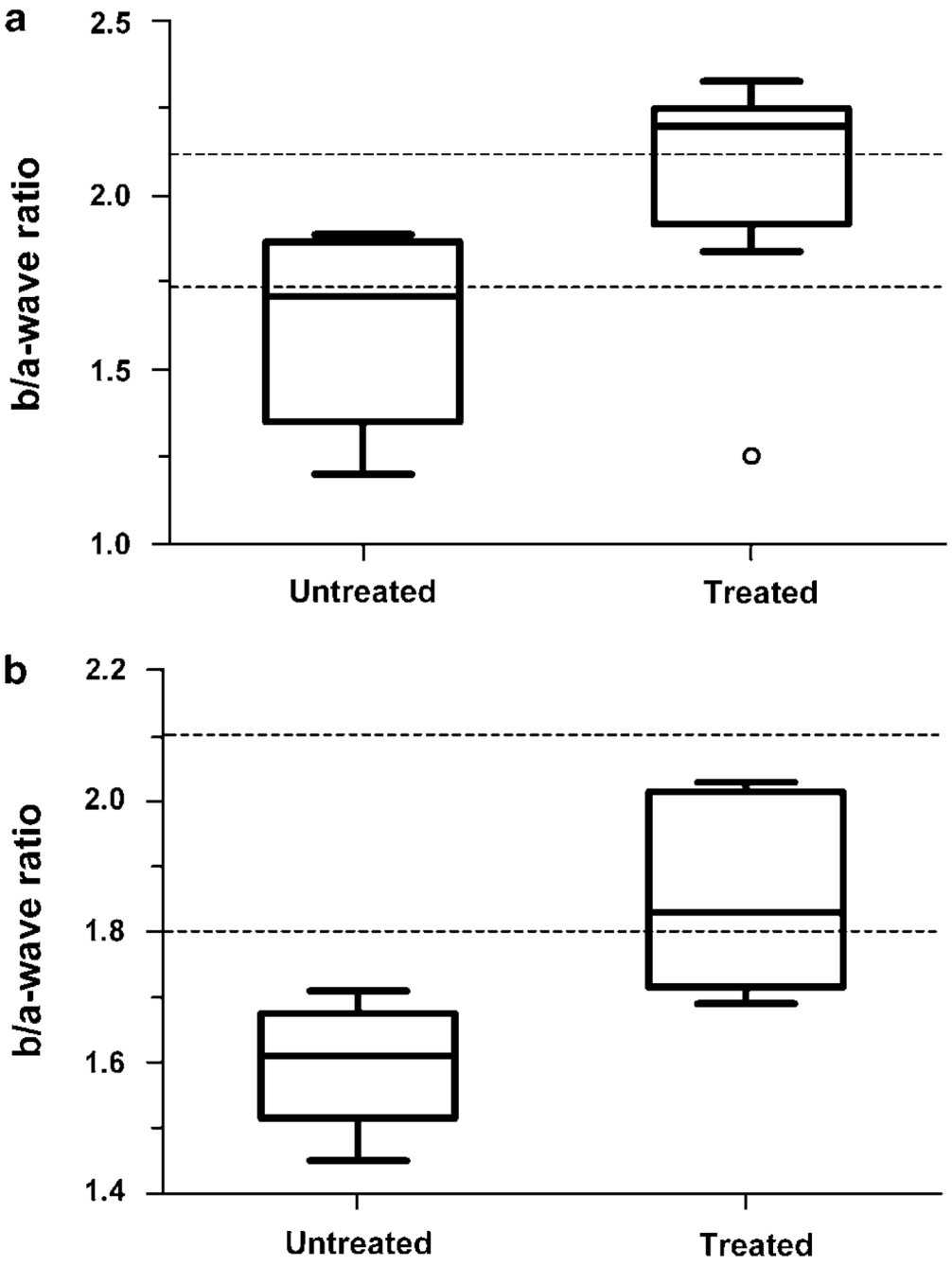

Figure 6.

Box and whiskers plot of b/a-wave ratios from Table 1 showing minimum and maximum, 25th and 75th percentile and median. (**a**) (Experiment 1) Retinoschisin knockout (*Rs1*-KO) mice were treated in both eyes (n = 8 eyes) with adeno-associated virus (AAV) 8-hRSp4 vector. Injections were performed at 6–7 weeks of age, and electroretinograms (ERGs) were recorded 11 weeks later. Age-matched untreated *Rs1*-KO mice were used as controls (n = 6 eyes), P = 0.04. Open circle is an outlier (1.5–3.0 times the interquartile range), which was included in the P-value calculation. (**b**) (Experiment 2) *Rs1*-KO mice were treated in one eye with AAV8-hRSp4 vector. Injections were done at 7–8 weeks of age, and ERGs were recorded 14.7–15.7

weeks later ($P = 0.012$, $n = 5$). The area between the dashed lines indicates the b/a-ratio range from a group of 39 wild-type animals.

Table 1

Prospective experiment 1: ERG of *Rs1*-KO mice treated with AAV8-hRSp4

Animal #	Eye	(b/a-wave) ratio[a]	Age at injection (week)	ERG: weeks after injection
4163	Untreated	1.89	Control	Control
	Untreated	1.63		
4165	Untreated	1.40	Control	Control
	Untreated	1.20		
4340	Untreated	1.86	Control	Control
	Untreated	1.79		
4226	Treated	2.25	6.6	11.1
	Treated	1.27[b]		
4227	Treated	1.84	6.6	11.1
	Treated	2.33		
4228	Treated	1.92	6.6	11.1
	Treated	2.20		
4303	Treated	2.20	7.3	11.1
	Treated	2.21		
Average[c]	Untreated	1.63 ± 0.28		
	Treated	2.03 ± 0.35		

[a] Ratio of b-wave amplitude to a-wave amplitude at 0.6 log cd-s m^{-2} flash intensity.

[b] Outlier included in calculation of average and *P* value but not in Figure 6 graph.

[c] Standard deviation of the mean.

Table 2

Prospective experiment 2: ERG of *Rs1*-KO mice treated with AAV8-hRSp4

Animal #	Eye	(b/a-wave) ratio[a]	Age at injection (week)	ERG: weeks after injection
4677	Untreated	1.64	7.4	14.7
	Treated	2.03		
4678	Untreated	1.61	7.4	15.7
	Treated	1.83		
4680[b]	Untreated	No ERG	7.4	Mouse died
	Treated	No ERG		
4683	Untreated	1.45	7.4	14.7
	Treated	1.74		
4687	Untreated	1.58	7.1	15.7
	Treated	2.00		
4689	Untreated	1.71	7.1	15.7
	Treated	1.69		
Average[c]	Untreated	1.60 ± 0.10		
	Treated	1.86 ± 0.15		

[a] Ratio of b-wave amplitude to a-wave amplitude at 0.6 log cd-s m^{-2} flash intensity.

[b] Animal died during anesthesia before ERG.

[c] Standard deviation of the mean.